Synthesis and Growth Mechanism of Bi_2S_3 Nanoribbons

Zhaoping Liu, Jianbo Liang, Shu Li, Sheng Peng, and Yitai Qian*[a]

Abstract: This article describes a facile solvothermal method by using mixed solvents for the large-scale synthesis of Bi_2S_3 nanoribbons with lengths of up to several millimeters. These nanoribbons were formed by a solvothermal reaction between Bi^{III}–glycerol complexes and various sulfur sources in a mixed solution of aqueous NaOH and glycerol. HRTEM (high-resolution transmission electron microscopy) and SAED (selective-area electron diffraction) studies show that the as-synthesized nanoribbons had predominately grown along the [001] direction. The Bi_2S_3 nanoribbons prepared by the use of different sulfur sources have a common formation process: the initial formation of $NaBiS_2$ polycrystals, which serve as the precursors to Bi_2S_3, the decomposition of $NaBiS_2$, and the formation of Bi_2S_3 seeds in the solution through a homogeneous nucleation process; the growth of Bi_2S_3 nanoribbons occurs at the expense of $NaBiS_2$ materials. The growth mechanism of millimeter-scale nanoribbons involves a special solid–solution–solid transformation as well as an Ostwald ripening process. Some crucial factors affect nanoribbon growth, such as, solvothermal temperature, volume ratio of glycerol to water, and the concentration of NaOH; these have also been discussed.

Keywords: bismuth · crystal growth · nanostructures · solvothermal synthesis · sulfide

Introduction

One-dimensional (1D) nanostructures (wires, rods, tubes, and ribbons) are expected to play an important role in fabricating nanoscale devices. As a result, the synthesis and characterization of 1D nanostructures have recently attracted extensive attention from a broad range of researchers.[1] In particular, much effort has been devoted to the controlled synthesis of 1D nanostructures from chalcogenides semiconductors due to their interesting physical properties, and their potential applications in fabricating optoelectric and thermoelectric nanoscale devices.[2] Main-group metals chalcogenides such as $A^V{}_2B^{VI}{}_3$ (A = As, Sb, Bi; B = S, Se, Te) group compounds are semiconductors and have applications in television cameras with photoconducting targets, thermoelectric devices, optoelectronic devices, and in IR spectroscopy.[3] Bismuth sulfide (Bi_2S_3) is a direct band-gap material with E_g of 1.3 eV, which makes it a useful material for photodiode arrays and photovoltaic converters.[4] It also belongs to a family of solid-state materials with applications in thermoelectric cooling technologies based on the Peltier effect.[5] The availability of Bi_2S_3 nanostructures with well-controlled morphology and dimension should be able to bring in new types of applications or enhance the performance of the currently existing device as a result of quantum-sized effects. So the synthesis of 1D nanostructures of Bi_2S_3 should be of great significance.

1D nanostructures of single-crystalline Bi_2S_3 have been prepared by various approaches, such as, a solvothermal (including hydrothermal) process,[6] template-directed procedure,[7] and a high-temperature evaporation method.[8] However, the quality of the as-synthesized 1D nanostructures of Bi_2S_3 from the previously reported solvothermal process in a single solvent (including water) was still unsatisfactory, because they were usually characteristic of nanorods with very small lengths (less than 5 μm) and low aspect ratios.[6] Some recent work of our group showed that solvothermal synthesis of some 1D nanostructures in mixed solvents, which were composed of two or more components (including water acting as one of the components), in some cases, were much more effective than that in a single solvent.[9] The as-prepared 1D nanostructures in the mixed solvents usually displayed uniform sizes, or high aspect ratios, and or, novel morphologies. Comparatively, the properties of the mixed solvents have a much larger scope, that can be adjusted by varying the components and their ratios, thus some optimum synthetic conditions may be achieved for the growth of high-quality 1D nanostructures. Recently, we have reported a very effective solvothermal synthetic method by using mixed solvents for the preparation of Bi_2S_3 nanoribbons

[a] Dr. Z. Liu, J. Liang, S. Li, S. Peng, Prof. Y. Qian
Structure Research Laboratory and
Department of Chemistry, University of Science and
Technology of China, Hefei, Anhui 230026 (P. R. China)
Fax: (+86) 551-360-7402
E-mail: liuzp@mail.ustc.edu.cn
ytqian@ustc.edu.cn

© 2004 Wiley-VCH Verlag GmbH & Co. KGaA, Weinheim
DOI: 10.1002/chem.200305481

with millimeter-scale lengths.[10] The growth of Bi_2S_3 nanoribbons was undergone in a mixed solution of aqueous NaOH and glycerol. In the previous study, we only used sodium thiosulfate ($Na_2S_2O_3$) as the sulfur source for the synthesis of Bi_2S_3 nanoribbons. After a series of experiments, we found that the sulfur sources for this synthesis are based on a wide range of sulfur materials, besides $Na_2S_2O_3$, such as elemental sulfur (S) powders, sodium sulfide (Na_2S), sodium dithionite ($Na_2S_2O_4$), carbon disulfide (CS_2), and so on. According to the features of these sulfur sources, they can be rationally divided into three groups: 1) sulfur compounds (e.g., $Na_2S_2O_3$) with good solubility in the aqueous NaOH–glycerol system, and releasing the S^{2-} ions only during the solvothermal process; 2) sulfur compounds (e.g., Na_2S and CS_2) that can directly give the S^{2-} ions or rapidly release the S^{2-} ions through the reaction with NaOH; and 3) elemental S in the form of solid powders. The studies on the synthesis of Bi_2S_3 nanoribbons by using sulfur sources with different features may provide more comprehensive insights for the formation mechanism of the nanoribbons. In this work, we present the synthesis of Bi_2S_3 nanoribbons by using three kinds of characteristic sulfur sources, and we pay more attention to understanding the formation process and growth mechanism of the nanoribbons, as well as, some crucial factors that affect nanoribbon growth.

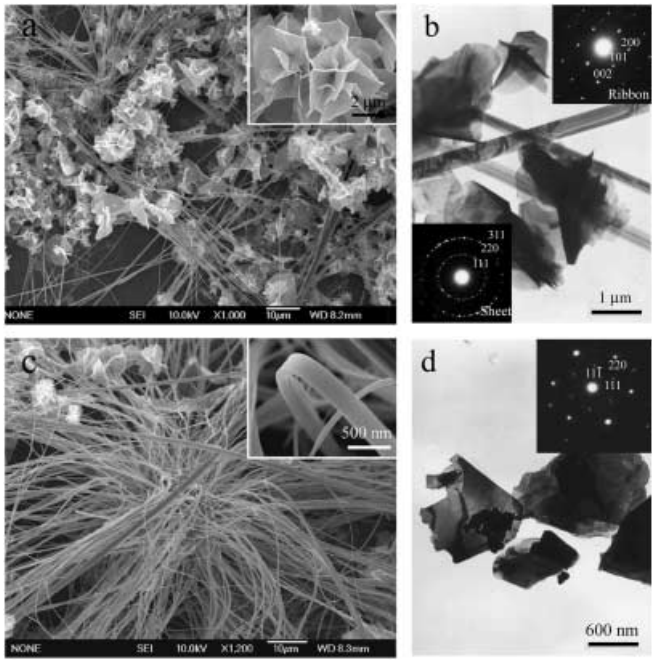

Figure 1. a) and c) SEM images of the samples prepared after heating for 3 and 12 h, respectively. The insets in Figure 1a and c give a high-magnification view of a petaloid sheet and a nanoribbon, respectively; b) TEM image of the same sample as shown in a. The upper right and lower left inset show the SAED of a nanoribbon and a petaloid sheet, respectively; d) TEM image of the $NaBiS_2$ sheets taken from products after 48 h. The inset displays the SAED pattern for the sheets.

Results

Synthesis of Bi_2S_3 nanoribbons by using thiosulfate as the sulfur source: In our previous report, Bi_2S_3 nanoribbons with millimeter-scale length have been successfully synthesized by using sodium thiosulfate ($Na_2S_2O_3$) as the sulfur source.[10] However, the formation process and growth mechanism of the nanoribbons have not been understood clearly. Therefore, here, we mainly investigate the evolution process of the nanoribbons by the use of representative sulfur sources. In the present studies, the intermediates are characterized in more detail by various techniques. Figure 1a and b shows the SEM and TEM image of a sample prepared after solvothermal treating for 3 h, respectively. As seen from these images, long nanoribbons and micro-sized sheet-like particles coexist in this sample. These nanoribbons have lengths of several hundreds of micrometers and widths of 50–300 nm. In a magnified view (inset of Figure 1a), one can see that these sheets are petaloid, and only several nanometers in thickness. SAED (selective-area electron diffraction) was used to characterize the phases of the two forms of the products. The upper right inset of Figure 1b shows the SAED pattern of a nanoribbon, while the lower left inset displays that of a sheet. The two SAED patterns identify the nanoribbons and the sheets as Bi_2S_3 single crystals, and $NaBiS_2$ polycrystals, respectively.

An increase in the growth time only led to the formation of more and longer nanoribbons (at the expense of the $NaBiS_2$ sheets). As shown in Figure 1c, the sample prepared after heating the solution for 12 h included a notable presence of uniform nanoribbons with lengths up to the scale of a millimeter. The inset in Figure 1c shows a typical image of a highly curved nanoribbon, which indicates that the as-synthesized nanoribbons have an excellent bending strength. Figure 1c also indicates that a few sheets were still present in the nanoribbons layers after a growth period of 12 h. In fact, the polycrystalline sheets of $NaBiS_2$ could also convert into single crystals, which were difficult to decompose Bi_2S_3, and these well-crystallized $NaBiS_2$ would deposit onto the bottom of the reaction container. It usually took about 48 h to completely convert all the polycrystalline sheets into Bi_2S_3 nanoribbons and $NaBiS_2$ single crystals. Figure 1d shows a typical TEM image of the sample taken from the deposit of products obtained after 48 h. The inset in Figure 1d shows an SAED pattern, which confirms these $NaBiS_2$ sheets are single crystalline.

Synthesis of Bi_2S_3 nanoribbons by using elemental S powders as the sulfur source: By using elemental sulfur powders as the sulfur source, we found that the morphology of the precursor ($NaBiS_2$) was very distinct from that of using the above-mentioned water-soluble sulfur sources. In the fist 1 h, nearly all the yellowish sulfur powders reacted, and were converted to black solids. A typical SEM image of this sample shows that the products consisted of quasi-spherical and uniform particles with diameters of 1–2 μm. Closer inspection reveals that these spheroids had innumerable pits on their surfaces, which looked like etched spheroids (see the inset of Figure 2a). Figure 3a shows the corresponding XRD (X-ray diffraction) pattern of this sample. All the peaks can be indexed to cubic structures of $NaBiS_2$ phase (JCPDS card, 8–406). However, judging from the weak and

 © 2004 Wiley-VCH Verlag GmbH & Co. KGaA, Weinheim

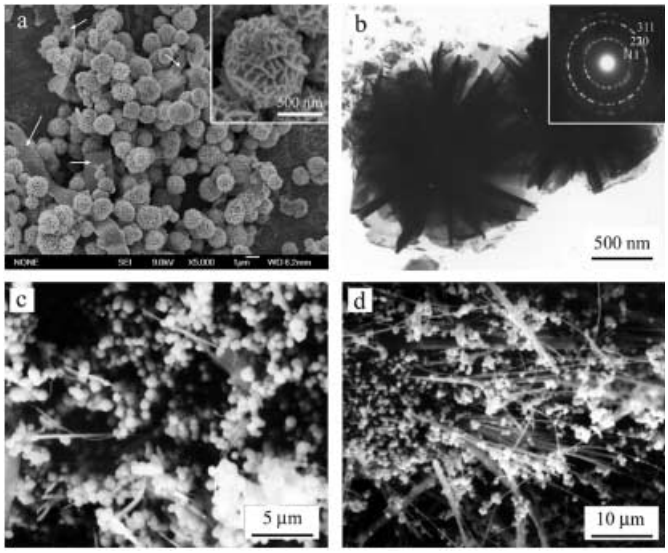

Figure 2. SEM images of the samples produced by the use of sulfur powders as the sulfur sources, and images taken after heating for various periods: a) 1 h, most of the particles are micrometer-sized spheroids, and sizes are relatively uniform; the inset in a) is the high-magnification view of an individual spheroids; c) 2 h, a few short nanoribbons can be observed; d) 3 h, considerable nanoribbons can be seen; b) a typical TEM image of the spheroids and SAED pattern (inset) for the spheroids.

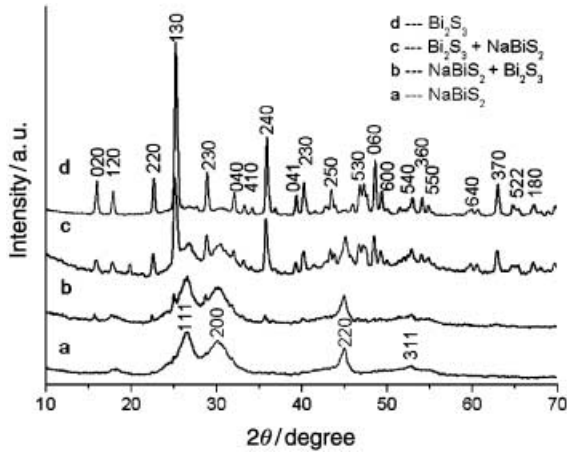

Figure 3. XRD patterns of the samples taken after heating for different reaction time: a) 1 h, b) 2 h, c) 3 h, and d) 24 h.

extensive broadening of the diffraction peaks in this XRD pattern, the etched spheroids of $NaBiS_2$ were poorly crystalline. A TEM image (Figure 2b) also depicts the structure of the particular etched spheroids. The inset shows an SAED pattern recorded from a spheroid, which indicates that it was polycrystalline; this agrees well with XRD results.

Based on the above investigations, the formation of etched spheroids of $NaBiS_2$ can be rationally interpreted as follows. Under solvothermal conditions, elemental S particles could immediately react with NaOH to give S^{2-} ions for the formation of a $NaBiS_2$ phase. The reaction initiated on the surface of the S particles, and seemed to be an erosion process. The released S^{2-} ions only occupy $^2/_3$ of the total S source, and some S^{2-} ions may have got into the solution. This may lead to the formation of $NaBiS_2$ polycrystals with special morphology, and much shrunk dimensions relative with those of the original S particles (usually 4–8 μm in sizes).

Once the polycrystalline $NaBiS_2$ particles had formed, the nucleation and growth of Bi_2S_3 1D nanostructures may have proceeded during the next solvothermal process. When the solvothermal process was extended to 2 h, a few short nanoribbons with lengths of several micrometers could be observed (see Figure 2c). We also found that some characteristic peaks of Bi_2S_3 phase, with weak intensity, appeared on the XRD pattern (Figure 3b). Therefore, it is possible that these nascent ribbonlike nanostructures were Bi_2S_3 crystals. After 3 h, substantial nanoribbons were generated, while the quantity of the etched spheroids was largely decreased, and many spheroids shrunk. This means the growth of Bi_2S_3 nanoribbons continuously proceeded through consuming the $NaBiS_2$ spheroids. In principle, extending the heating time elongated the nanoribbons and consumed $NaBiS_2$ spheroids. This tendency could also be interpreted by a contrast in the variation of peak intensity in the XRD patterns (Figure 3a–d), in which the characteristic peaks of Bi_2S_3 were largely intensified, and those of $NaBiS_2$ were weakened as the heating time was increased; the peaks of $NaBiS_2$ eventually disappeared after a 24 h heating process.

After a 24 h solvothermal process, a large amount of nanoribbons were produced, of which, floated on the top of the reaction container. A typical SEM image (Figure 4a) shows that these nanoribbons are usually 100–250 nm wide, 20–60 nm thick, and up to several millimeters long. No

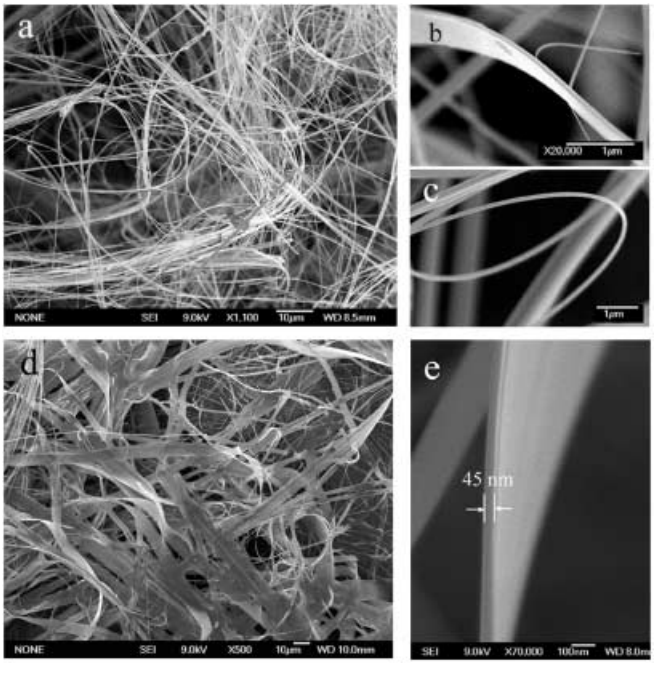

Figure 4. a) SEM image of the final product produced after a 24 h heating process, which revealed the high-purity and uniform morphology of the nanoribbons; b) and c) display the characteristic features of nanoribbons and nanowires, respectively; d) SEM image of some wide nanoribbons with widths of up to 10 μm; e) shows the side surface of a wide nanoribbon.

© 2004 Wiley-VCH Verlag GmbH & Co. KGaA, Weinheim

etched spheroids or other particles can be observed in the Bi_2S_3 layers. A SEM image in high-magnification view (Figure 4b) clearly depicts a ribbon with a typical rectangular cross-section. Some nanowires were also observed (see Figure 4c). In addition, we also noticed that a few very wide ribbons were generated, and they floated on the upside of the Bi_2S_3 layers. The widths of these wide ribbons were usually several micrometers (see Figure 4d), and thicknesses of only 40–60 nm (see Figure 4e). Since some short and wide ribbonlike structures were also observed in the initial products (indicated by arrows in Figure 2a), it is possible that nucleation of wide nanoribbons starts in the initial stage of the solvothermal process.

Synthesis of Bi_2S_3 nanoribbons by using sulfides as the sulfur source: Differing from the $Na_2S_2O_3$ and elemental S, Na_2S can directly give S^{2-} ions. Once it was added into the reaction solution, a black turbid suspension formed immediately. To identify the solid particles that formed in the resulted suspension, the suspension was centrifuged to collect a solid sample, and then characterized by XRD. The XRD pattern (Figure 5a(I)) indicates that the initial product

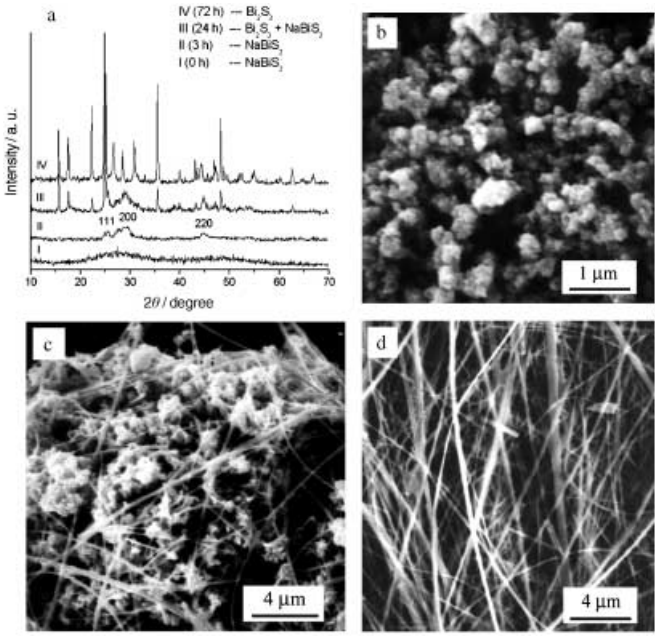

Figure 5. XRD patterns a) of the samples prepared by using sulfides as the sulfur source at different periods of heating time: I) 0, II) 3, III) 24, and IV) 72 h. SEM images of the samples taken after heating for various time: b) 3, c) 24, and d) 72 h.

seemed to be an amorphous $NaBiS_2$ phase. After solvothermally treating the resulted suspension for 3 h, polycrystalline $NaBiS_2$ was obtained (see Figure 5a(II)). The SEM image (Figure 5b) shows a sample, that consisted of aggregated particles with sizes of several hundred of nanometers. It could be anticipated that Bi_2S_3 nanoribbons would grow from this mixture. However, we found the evolution process of the nanoribbons was much slower than that of using $Na_2S_2O_3$ or elemental S as the sulfur sources. The XRD pattern (Figure 5a(III)) of a sample taken after a 24 h solvothermal process depicts the $NaBiS_2$ phase, that still coexists with the Bi_2S_3 phase. The SEM image (Figure 5c) also shows that the sample consisted of a certain amount of aggregated particles. In this case, it took over 72 h to form pure nanoribbons and consume the mass of $NaBiS_2$ particles. As shown in Figure 5d, bulk, pure nanoribbons were formed. The XRD pattern (Figure 5a(IV)) also indicates the pure Bi_2S_3 phase.

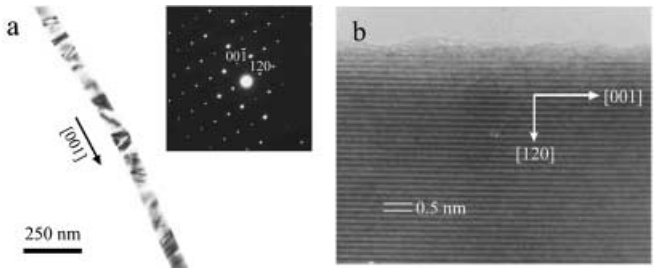

Figure 6. a) The TEM image and SAED pattern obtained from an individual nanoribbon; b) HRTEM image recorded near the edge of the particular Bi_2S_3 nanoribbon along the direction perpendicular to the wide surface of the nanoribbon.

Structural characterization of as-synthesized Bi_2S_3 nanoribbons: The structural information of as-synthesized Bi_2S_3 nanoribbons has been characterized by using SAED and HRTEM (high-resolution transmission electron microscopy). Figure 6a shows a representative TEM image of an individual nanoribbon with a width of about 65 nm. The inset displays a typical SAED pattern that was recorded from this nanoribbon, and all diffraction spots were indexed to the orthorhombic phase of Bi_2S_3. This SAED pattern also reveals that the nanoribbon grew along the [001] direction. An HRTEM image taken near the edge along the length of this nanoribbon is shown in Figure 6b. As seen from the image, this particular nanoribbon is a structurally uniform single-crystal. The observed interplanar spacing is about 0.5 nm, which corresponds to the separation between the {120} lattice planes of the Bi_2S_3 phase. Diffraction patterns taken from different parts of this ribbon show exactly the same pattern without further tilting the sample; this indicates the single crystallinity of the whole ribbon. More individual nanoribbbons have also been examined by this method, and the resulting diffraction patterns suggest that most of ribbons grow along the [001] direction, although, we have observed some nanoribbons that may have a growth along the $[\bar{2}10]$ direction in our previous report.[10] In addition, the usually strong reflection peaks ($hk0$), and weak peaks (hkl) ($l \neq 0$) were seen in the XRD pattern (Figure 3d), which suggests that the as-synthesized Bi_2S_3 nanoribbons might lie on the surface of the silicon wafer, and have a preferential origination of the [001] direction. This further confirms the results of both HRTEM and SAED studies.

 © 2004 Wiley-VCH Verlag GmbH & Co. KGaA, Weinheim

Discussion

Formation process and growth mechanism of Bi_2S_3 nanoribbons: From the above experimental results, although the sulfur sources are different, the formation of Bi_2S_3 nanoribbons has been observed to follow in a similar growth process. This common process can be reasonably elucidated as the following three stages: i) the formation of $NaBiS_2$ polycrystals by the reaction between the sulfur sources and the Bi^{III}–glycerol complexes at the beginning of the solvothermal process; ii) the decomposition of $NaBiS_2$, and the successive nucleation of Bi_2S_3 nanocrystals; and iii) the continuous growth of Bi_2S_3 nanoribbons at the expense of $NaBiS_2$ materials. Since all these sulfur sources can give S^{2-} ions directly, or under the solvothermal conditions, the chemical reaction involved in the entire synthesis of Bi_2S_3 nanoribbons can be formulated, as shown in Equations (1)–(3).

$$Bi(C_3O_3H_5) + 2\,S^{2-} + Na^+ + 3\,H_2O \rightarrow NaBiS_2 + C_3O_3H_8 + 3\,OH^- \quad (1)$$

$$2\,NaBiS_2 \leftrightarrow 2\,Na^+ + Bi^{3+} + 2\,S^{2-} \quad (2)$$

$$2\,Bi^{3+} + 3\,S^{2-} \leftrightarrow Bi_2S_3 \quad (3)$$

The $Bi(C_3O_3H_5)$ complexes are first formed before the solvothermal process through the reaction between Bi^{3+}, OH^-, and glycerol ($C_3O_3H_8$).[11] It can be concluded that the whole process involves a special solid–solution–solid transformation, in which the decomposition of the $NaBiS_2$ polycrystals gives Bi_2S_3 units for the nucleation and growth of Bi_2S_3 nanoribbons. Therefore, the $NaBiS_2$ polycrystals can be regarded as a crucial precursor for the formation of Bi_2S_3 nanoribbons. However, the morphologies of the precursors by using different sulfur sources are very different. The experimental observations have revealed they display morphologies in the form of petaloid sheets for $Na_2S_2O_3$, etched spheroids for S powders, and aggregated particles for Na_2S. These precursors may have different free-energies due to the difference in their forms. For instance, the aggregated particles of $NaBiS_2$ may have a lower free-energy relative to the petaloid sheets and the etched spheroids. This leads to decomposition of the precursors at a lower rate. As a result, by using sulfides as the sulfur sources, a longer solvothermal time is needed for the bulk formation of nanoribbons.

Although our previous observations showed some Bi_2S_3 seeds were generated on petaloid sheets,[10] our present SEM, TEM, and SAED studies suggest that the majority of Bi_2S_3 seeds are possibly formed in solution through a homogenous nucleation-process. Based on the observations of the initial products, we find that the initially formed ribbons are not attached on the surfaces of both the petaloid sheets (see Figure 1a and b and the etched spheroids (see Figure 2c and d). The nucleation of nanoribbons does not seem to initiate on the surface of these etched spheroids, but is more likely to occur in homogenous solution. Under solvothermal conditions the Bi_2S_3 units are generated in solution through the decomposition of $NaBiS_2$ polycrystals, and then through a condensation process they will form small sheets of Bi_2S_3, which will be used as the seeds for the growth of 1D nanostructures with ribbonlike morphology.

It is known that Bi_2S_3 has a lamellar structure with linked Bi_2S_3 units, which form infinite chains parallel to the *c* axis ([001] direction).[12] This anisotropic structure suggests that Bi_2S_3 has a strong tendency toward 1D growth along the [001] direction, which may lead to the formation of 1D nanostructures (such as nanowires and nanorods). Our SAED and HRTEM studies also confirm the as-prepared nanoribbons had predominately grown along the [001] direction. In previous reports, 1D nanostructures of Bi_2S_3 have been synthesized through a solvothermal method by using various solvents, such as water,[6a] ethanol,[6b] ethylene glycol,[6c] diethylene glycol,[6d] and so forth. However, these 1D nanostructures prepared in a single solvent had very short lengths (usually lower than 5 μm), and they could be classed as nanorods. In our present synthesis, the as-obtained Bi_2S_3 nanoribbons have a millimeter-scale length. What is the driving force for the formation of the ultra-long nanoribbons? It is believed that the as-used mixed solvents should be responsible for this. In the mixture of aqueous NaOH and glycerol, a stable complex $Bi(C_3O_3H_5)$ is formed,[11] so the solubility of Bi_2S_3 can be largely increased in this particular solution system under solvothermal conditions. This will ensure a relatively higher concentration of Bi_2S_3 units, and higher chemical potential in the solution; this is believed to be favorable for the growth of 1D nanostructures.[13] As a result, the growth of Bi_2S_3 1D nanostructures along the [001] direction should be at a high rate. During a continuous solvothermal process, some shorter nanoribons may redissolve and contribute to the growth of longer ones through a process known as Ostwald ripening.[14] This allows us to obtain nanoribbons with lengths of up to several millimeters.

Crucial factors affecting nanoribbon growth: In principle, the growth process of Bi_2S_3 nanoribbons would not continue until all the $NaBiS_2$ polycrystals were completely consumed, and only long nanoribbons survived. Nevertheless, our previous investigations have also revealed that the transformation of $NaBiS_2$ polycrystals mainly took place in two ways: decomposition and crystallization.[11] The decomposition of $NaBiS_2$ could give Bi_2S_3 units, whereas the crystallization generated single crystals of $NaBiS_2$. Therefore, it was impossible to convert all $NaBiS_2$ material into Bi_2S_3 nanoribbons. In general, the yield of Bi_2S_3 nanoribbons was up to 90% (according to the amount of $Bi(NO_3)_3{\cdot}5\,H_2O$ input). The longer nanoribbons that were formed would automatically float on the upside of the reaction container, and conveniently self-separate from the $NaBiS_2$ deposit, and thus the unconverted $NaBiS_2$ could not lead to impurities in the nanoribbon products. Further investigations found that the solvothermal temperature had a great influence on the crystallization of $NaBiS_2$. At 200 °C, the reaction only gave $NaBiS_2$ single crystals. When the reaction was processed under certain reflux conditions (at 118 °C), all the $NaBiS_2$ could be converted to Bi_2S_3, and the final products only consisted of Bi_2S_3 nanoribbons. Theses results suggest that the crystallization of $NaBiS_2$ was accelerated as the temperature increased. However, the Bi_2S_3 nanoribbons prepared under

© 2004 Wiley-VCH Verlag GmbH & Co. KGaA, Weinheim

the reflux conditions had lengths of only 10–20 μm. This could ascribe to the relatively lower concentration of Bi_2S_3 units at a lower solvothermal-temperature. Therefore, it is important to select an optimum temperature for the formation of millimeter-scale nanoribbons in high yield. We found that the suitable temperatures ranged from 140 to 180 °C. By running the solvothermal reaction in this temperature range, bulk Bi_2S_3 nanoribbons with lengths of up to several millimeters could be successfully produced.

It is believed that the physical and chemical properties of the solvent can influence the solubility, reactivity, and diffusion behavior of the regents and the intermediate. In our synthesis system, the properties of the mixed solvent can be easily adjusted by varying the ratios of the two components (glycerol and water). Therefore, it is supposed that the volume ratio of glycerol to water has a great influence on the growth of Bi_2S_3 nanoribbons. We thus investigated this synthesis parameter in detail, and found that a high yield of Bi_2S_3 nanoribbons was formed only in a suitable volume ratio range of between 1:1 and 2:1. As the ratio was increased beyond 3:1 or decreased to 1:3, only a few Bi_2S_3 nanoribbons could be formed, and $NaBiS_2$ particles were obtained as the major product. This may be because a lower volume ratio of glycerol to water led to a lower concentration of Bi_2S_3 units in the solvothermal reaction system, and also an overhigh ratio resulted in a very low-diffusion coefficient of the Bi_2S_3 units due to high viscosity. The two cases (both the low concentration and the low diffusion coefficient of Bi_2S_3 units) were unfavorable for the growth of Bi_2S_3 nanoribbons.

We also investigated the influence of NaOH concentration on the growth of Bi_2S_3 nanoribbons. The studies were focused on synthesis by using thiosulfate as the sulfur source. In these studies, the solvothermal reaction was carried out in a volume ratio of glycerol/water 2:1 at a temperature of 160 °C for 24 h. We found that the concentration of NaOH in the range of 1.5–3.0 M was favorable for the formation of ultra-long Bi_2S_3 nanoribbons with a high yield. At 0.5 M of NaOH solution, the product was dominated by Bi_2S_3 particles with irregular morphologies, and no $NaBiS_2$ phase could be detected. As the concentration of NaOH was increased beyond 3 M, $NaBiS_2$ particles were obtained as the major product, and only the $NaBiS_2$ phase could be formed at 4.5 M of NaOH solution. These results may be rationally explained in Equation (2), in which the concentration of Na^+ had a great influence on the decomposition rate of $NaBiS_2$. Apparently, at a higher concentration of Na^+, the decomposition of $NaBiS_2$ was more difficult, and this led to more $NaBiS_2$ polycrystalline particles crystallized as single crystals. At a very low concentration of Na^+, the $NaBiS_2$ could decompose very rapidly, and this would lead to a very high supersaturation of Bi_2S_3 units in the reaction system; this was unfavorable for the growth of Bi_2S_3 nanoribbons.

Conclusion

We have demonstrated a facile and versatile solvothermal method for large-scale synthesis of Bi_2S_3 nanoribbons in mixed solvents of glycerol and water. These nanoribbons were characterized as having millimeter-scale lengths and high purity. Although the sulfur sources are different, Bi_2S_3 nanoribbons have undergone a similar formation process, which is characteristic of the formation of $NaBiS_2$ precursor polycrystals, and the growth of Bi_2S_3 nanoribbons through a solid–solution–solid transformation, as well as, an Ostwald-ripening process. The suggested growth mechanism is in good agreement with our experimental results. Compared with solvothermal synthesis in a single solvent, the advantages of our method for the preparation of chalcogenide nanoribbons lies in its simplicity, high yield, high purity, and low processing temperature. Therefore, it offers a more attractive and convenient approach for large-scale synthesis of chalcogenide nanoribbons. The present results show that the solvothermal synthetic route, by using mixed solvents, may provide a more promising approach for rationally designing 1D nanostructural materials. Since we have detected that Bi_2S_3 nanoribbons had signal photovoltaic spectrum in the red-light region,[10] the as-synthesized nanoribbons may have a promising application in photovoltaic converters or other photoelectronic nanodevices.

Experimental Section

Chemicals and materials: All the chemicals were of analytical grade and used without further purification. Deionized water was used throughout. Bismuth nitrate ($Bi(NO_3)_3{\cdot}5H_2O$), sodium hydroxide (NaOH), glycerol ($C_3O_3H_8$), sodium thiosulfate ($Na_2S_2O_3{\cdot}5H_2O$), elemental sulfur powders (S), and sodium sulfides ($Na_2S{\cdot}5H_2O$), which were all purchased from Shanghai Chemical Regents Company.

Synthesis of Bi_2S_3 nanoribbons: In a typical procedure, $Bi(NO_3)_3{\cdot}5H_2O$, NaOH, and the sulfur compound were introduced into a mixture of distilled water and glycerol to give the final concentration of 50 mM Bi^{III}, 2 M NaOH, and 100 mM sulfur compound; the volume of glycerol to water was in the ratio of 2:1. Then the mixture (45 mL) was transferred into a Teflon-lined autoclave (55 mL capacity). The autoclave was maintained at 160 °C for 24 h (or 72 h for Na_2S), and then cooled to room temperature naturally. It was found that a large quantity of dark gray wirelike particles floated on the top of the solution, and a small quantity of black-brown particles deposited on the bottom of the autoclave. The two products with different forms were carefully collected and washed with distilled water. The two products were then dried in a vacuum oven at 60 °C for 4 h.

Characterization: The X-ray diffraction (XRD) analysis was performed by using a Rigaku (Japan) D/max-γA X-ray diffractionmeter equipped with graphite monochromatized $Cu_{K\alpha}$ radiation ($\lambda = 1.54178$ Å). The SEM images were taken with a scanning electron microscope (Hitachi X-650) and a field-emission-scanning electron microscope (JEOL-6300F, 15 kV). The TEM images and SAED patterns were recorded on a Hitachi 800 TEM, and were performed at 200 kV. The HRTEM images and the corresponding SAED patterns were taken on a JEOL 2010 high-resolution TEM performed at 200 kV.

Acknowledgement

This work was supported by National Natural Science Foundation of China and the 973 Project of China.

[1] a) Y. Huang, X. F. Duan, Q. Q. Wei, C. M. Lieber, *Science* **2001**, *291*, 630; b) D. Vion, A. Aassime, A. Cottet, P. Joyez, H. Pothier, C.

 © 2004 Wiley-VCH Verlag GmbH & Co. KGaA, Weinheim

Urbina, D. Esteve, M. H. Devoret, *Science* **2002**, *296*, 886; c) Z. W. Pan, Z. R. Dai, Z. L. Wang, *Science* **2001**, *291*, 1947; d) M. H. Huang, S. Mao, H. Feick, H. Q. Yan, Y. Y. Wu, H. Kind, E. Weber, R. Russo, P. D. Yang, *Science* **2001**, *292*, 1897; e) B. Gates, B. Mayers, B. Cattle, Y. N. Xia, *Adv. Funct. Mater.* **2002**, *12*, 219; f) X. M. Sun, Y. D. Li, *Chem. Eur. J.* **2003**, *9*, 2229.

[2] a) Y. W. Jun, S. M. Lee, N. J. Kang, J. W. Cheon, *J. Am. Chem. Soc.* **2001**, *123*, 5150; b) C. Ma, D. Moore, J. Li, Z. L. Wang, *Adv. Mater.* **2003**, *15*, 228; c) L. S. Li, A. P. Alivisatos, *Adv. Mater.* **2003**, *15*, 408; d) Y. Feldman, E. Wasserman, D. A. Srolovitz, R. Tenne, *Science* **1995**, *267*, 222; e) Z. A. Peng, X. G. Peng, *J. Am. Chem. Soc.* **2001**, *123*, 183.

[3] D. Arivuoli, F. D. Gnanam, P. Ramasamy, *J. Mater. Sci. Lett.* **1998**, *7*, 711.

[4] a) D. D. Miller, A. Heller, *Nature* **1976**, *262*, 280; b) P. K. Mahapatra, C. B. Roy, *Sol. Cells* **1982/83**, *7*, 225; c) J. M. Schoijet, *Sol. Energy Mater.* **1979**, *1*, 43.

[5] P. Boudjouk, M. P. Remngton, Jr., D. G. Grier, B. R. Jarabek, G. J. McCarthy, *Inorg. Chem.* **1998**, *37*, 3538.

[6] a) W. X. Zhang, Z. H. Yang, X. M. Huang, S. Y. Zhang, W. C. Yu, Y. T. Qian, Y. B. Jia, G. E. Zhou, L. Chen, *Solid State Commun.* **2001**, *119*, 143; b) S. H. Yu, Y. T. Qian, L. Shu, Y. Xie, L. Yang, C. S. Wang, *Mater. Lett.* **1998**, *35*, 116; c) G. Z. Sheng, D. Chen, K. B. Tang, F. Q. Li, Y. T. Qian, *Chem. Phys. Lett.* **2003**, *370*, 334; d) D. B. Wang, M. W. Shao, D. B. Yu, G. P. Li, Y. T. Qian, *J. Cryst. Growth* **2002**, *243*, 331.

[7] X. S. Peng, G. W. Meng, J. Zhang, L. X. Zhao, X. F. Wang, Y. W. Wang, L. D. Zhang, *J. Phys. D* **2001**, *34*, 3224.

[8] C. H. Ye, G. W. Meng, Z. Jiang, Y. H. Wang, G. Z. Wang, L. D. Zhang, *J. Am. Chem. Soc.* **2002**, *124*,15180.

[9] a) Y. Jiang, B. Xie, S. Yuan, Y. Wu, H. Huang, Y. T. Qian, *J. Solid State Chem.* **2002**, *167*, 28; b) D. B. Yu, D. B. Wang, S. Y. Zhang, X. M. Liu, Y. T. Qian, *J. Mater. Chem.* **2002**, *12*, 103; c) M. S. Mo, J. H. Zeng, X. M. Liu, W. C. Yu, S. Y. Zhang, Y. T. Qian, *Adv. Mater.* **2002**, *14*, 1658.

[10] Z. P. Liu, S. Peng, Q. Xie, Z. K. Hu, Y. Yang, S. Y. Zhang, Y. T. Qian, *Adv. Mater.* **2003**, *15*, 936.

[11] *Chemistry Dictionary (Chinese)* (Eds.: Y. D. Gu, Y. Xia), Shanghai Dictionary Publishing, **1989**, p. 634.

[12] J. Black, E. M. Conwell, L. Seigle, C. W. Spencer, *J. Phys. Chem. Solids* **1957**, *2*, 240.

[13] a) Z. A. Peng, X. G. Peng, *J. Am. Chem. Soc.* **2001**, *123*, 1389; b) X. G. Peng, *Adv. Mater.* **2003**, *15*, 459.

[14] a) E. Matijevic, *Chem. Mater.* **1993**, *5*, 412; b) A. R. Roosen, W. C. Carter, *Physica A* **1998**, *261*, 232.

Received: August 27, 2003 [F5481]

© 2004 Wiley-VCH Verlag GmbH & Co. KGaA, Weinheim